

## RESEARCH ARTICLE

# Improved compensation of terrain topography effects on SAR images using cross-correlation matching

Mikael El Ouazzani\*      Maximilien Soviche\*

SUPERVISOR: Ludovic Villard †

May 25, 2020

### Abstract

Improving the compensation of terrain topography effects on Synthetic Aperture Radar (SAR) backscattering coefficients proves to be a challenging issue for decades, especially with longer wavelengths at L or P-band for which ground contributions can be very significant. Indeed, there exists numerous compensation methods with variable performances mainly due to the local acquisition geometry for both SAR image and Digital Surface Model (DSM) of the underlying ground effect, but none of them can provide a complete correction (free of significant residuals). We aimed to develop an improved co-registration method between P-band SAR intensity image and the compensating function mainly derived from the local incidence. Our method is based on Normalized Cross-Correlation (NCC) template matching applied to overlapped patches of data. Such approach enables to generate a vector field representing the displacement between two images. The proposed approach has been tested with P-band SAR data resulting from the TropiSAR campaign conducted in French Guiana during phase A (feasibility study) activities of the upcoming BIOMASS mission. Based on a state-of-the-art backscattering coefficient and on in-situ reference AGB data for almost 85ha of forest plots, our method accounting for the optimized matching enables to significantly increase their mutual correlation (16 to 24% increase) and can be achieved efficiently without the need of human supervision or a-priori knowledge and training dataset, paving the way for further study cases and promising improvement in terms of AGB retrieval.

---

<sup>0</sup>National Institute of Applied Science (INSA) Toulouse, Department of Applied Mathematics, 31400 Toulouse, France; elouazza@etud.insa-toulouse.fr (M.E.); soviche@etud.insa-toulouse.fr (M.S.)

<sup>†</sup>Centre d'Etudes Spatiales de la Biosphère, 31400 Toulouse, France; ludovic.villard@cesbio.cnes.fr

# Contents

<b>List of Figures</b>	<b>3</b>
<b>1 Introduction</b>	<b>4</b>
<b>2 Methodology</b>	<b>5</b>
2.1 Template matching using cross-correlation . . . . .	5
2.1.1 Fundamentals . . . . .	5
2.1.2 Template matching based on cross correlation . . . . .	5
2.1.3 Template matching implementation . . . . .	6
2.2 From template matching to displacement field . . . . .	7
2.2.1 Creating a vector field from multiple template matching results . . . . .	7
2.2.2 Superimpose images with a displacement field . . . . .	8
2.2.3 Overlapping patches for improved accuracy . . . . .	8
<b>3 Study case of the Paracou test site with TropiSAR data</b>	<b>9</b>
3.1 Test site features . . . . .	9
3.2 Matching DEM image and SAR intensity image . . . . .	9
3.3 Estimating image matching impact on SAR intensity to AGB correlation . . . . .	11
3.4 Tuning parameters . . . . .	12
<b>4 Conclusion and further prospects</b>	<b>12</b>
<b>5 Acknowledgment</b>	<b>13</b>
<b>References</b>	<b>14</b>

## List of Figures

1	Template matching of a template $g$ onto a reference $f$ . . . . .	6
2	Template matching . . . . .	6
3	Vector field obtained thanks to patch-wise template matching protocol . . . . .	7
4	Template matching setting of $g$ onto $f$ for a situation with constraint set $X$ . . . . .	7
5	Template matching protocol . . . . .	8
6	Experimental data from TropiSAR data and initial compensation image based on angles calculation from SRTM DEM. . . . .	9
7	Experimental results and comparison of initial and optimized matching of P-band SAR image with DEM image in the focus zone. . . . .	10
8	P-band backscatter intensity (dB) in terms of AGB $\log_{10}(t/\text{ha})$ . . . . .	11

# 1 Introduction

Today forest Above Ground Biomass (AGB) worldwide estimates are the main limitations in the modeling of Earth system carbon balance [1]. Although quantifying AGB at global scale plays a key role in improving our understanding of the global carbon cycle, none of the current spaceborne observations are truly adapted to this challenging issue. Most operating in-orbit platforms use L-band SAR for their measurements. L-band (1 - 2 GHz) has proven its advantages for estimating AGB during missions such as ALOS/PALSAR [2] but is not suitable for dense tropical forest since its wavelength is too low to ensure a sufficient penetration and sensitivity to catch a significant fraction of woody biomass, as shown in [3], [2]. Indeed, L-band sensors are only sensitive to the uppermost level of the forest canopy (mainly leaves) whereas the goal is to estimate dry biomass (trunk, primary or secondary branches).

To address this challenging issue, the European Space Agency (ESA) has selected the so-called BIOMASS mission as its seventh Earth Explorer mission in 2013, based on the very first use from space of a P-band SAR [1]. P-band (435 MHz), which was until recently allocated for military applications, enables a higher penetration through the dense forest canopy (superior to 300 t/ha) resulting in a better sensitivity to forest AGB. However, its penetration capacity makes it more sensitive to the underlying terrain, so that backscatter contributions from the ground are liable to impair the relation between radar intensity and forest AGB if those effects are not properly accounted for. Therefore, P-band potential for AGB retrieval cannot be capitalized on without accounting for the problem of backscatter contribution. Yet, pre-process data by compensating topography induced backscattered contribution has shown to be a complex task due to numerous scattering mechanisms [4]. In this paper we focus on geometrical model-based methods. These consist in assessing incidence angles and intercepted volume with respect to local slopes, then applying a correcting factor to the data. This type of approach implies an accurate matching between P-band backscatter intensity and Digital Elevation Models (DEM). There exists numerous image matching methods. Some constraints are the need for human help to place key points on the images (anchorage methods) [5], [6] or the need for large training datasets (supervised learning methods) [7].

Given these constraints, we aimed to develop an easy to implement image matching method using a template matching algorithm based on normalized cross-correlation (NCC) [8]. At this stage, P-band SAR images from the TropiSAR campaign provide us a very rich database with sufficient terrain topography for this study. The goal of this campaign was to evaluate the P-band radar imaging over tropical forest in anticipation of the BIOMASS mission [9]. This campaign took place in French Guiana and among the three overflowed test sites we have selected the Paracou one in order to get a wide range of terrain topography types and forest plots where reference in-situ values of AGB could be used. For this campaign, a georeferencing look-up table have been provided in order to select an arbitrary height (DSM based or other) in the conversion from radar to ground geometries. In our study, height values from the SRTM 30m DEM have been used for this georeferencing process, hence a possible shift due to forest height which originate the differences between a C-band DEM and the corresponding DTM (Digital Terrain Model).

Our approach is straight forward: we use NCC to accomplish template matching on overlapping subsets (or patches) of our data. Each template matching produces a displacement vector between the topography image and the P-band backscatter image. Iterating the process over the whole data (or a designated region of it) produces a displacement field that we use to compensate ground backscattering contribution. We compensate data by averaging the displacement vectors and then applying a linear translation of that calculated average on the P-band backscatter intensity image.

Using in-situ AGB measurements in different ROI in the Paracou site, we managed to assess the quality of our matching method. Backscatter-AGB relationship is modeled by a power-law [10], which goodness of fit can be cross-compared between the initial and the optimized matching.

In this paper we first discuss cross-correlation methods applied to template matching, then we explain our process to build an image matching method from it. The second section contains implementation testing and benefits in terms of goodness of fit between intensity and in-situ AGB. Finally we discuss potential improvements of the method and further tests to consolidate our findings.

## 2 Methodology

Our matching problem can be reformulated as correctly superimposing two images of the same size but taken from different sources i.e. find an accurate displacement field between the two images. A common and accurate way to achieve this is by using control points methods, main drawback being the need for human intervention [5], [6]. Another class of techniques rely on learning algorithms, which can produce very good results only if sufficient amount of training data is provided. The BIOMASS mission use-case does not allow for human intervention methods nor data hungry training methods.

In this paper we propose to use template matching on overlapping patches of the images, using Normalized Cross-Correlation (NCC), to calculate a displacement field between them. In the following section we describe the process to adapt NCC template matching to multi modal image matching.

### 2.1 Template matching using cross-correlation

Let us first recall what cross-correlation is and then discuss on its template matching application.

#### 2.1.1 Fundamentals

The cross-correlation function is a fundamental tool for comparing two signals. It measures the similarity of a signal  $f$  regarding a lagged signal  $g$ . It can be interpreted as a sliding dot-product which provides a similarity indicator for a given lag  $\tau$  of one signal with respect to the other.

$$(f \star g)(\tau) = \int_{-\infty}^{\infty} \overline{f(t)}g(t + \tau) dt \quad (1)$$

This base principle can be applied in the same way for template matching in images.

#### 2.1.2 Template matching based on cross correlation

Let us suppose we want to match a given template image  $g$  of size  $n \times m$  onto an image  $f$  of size  $M \times N$  with  $N > n$  and  $M > m$  (see Figure 2). The standard approach to template matching is to calculate a similarity degree for every possible position of the template  $g$  onto a the reference  $f$ . The maximum similarity position gives the template position in the reference image. Although other similarity indicators exist, including the Sum of Absolute Differences (SAD) or the Sum of Squares Differences (SDD), Normalized Cross-Correlation (NCC) is a better choice as it is the most robust one [8].

Base formula for 2d cross-correlation evaluated on point  $(u, v)$  is given by

$$c(u, v) = \sum_{x,y} f(x, y) \cdot g(x - u, y - v) dx dy \quad (2)$$

which gives us the NCC indicator when it is normalized :

$$\gamma(u, v, f, g) = \frac{\sum_{x,y} [f(x, y) - \bar{f}_{u,v}] [g(x - u, y - v) - \bar{g}]}{\left\{ \sum_{x,y} [f(x, y) - \bar{f}_{u,v}]^2 \sum_{x,y} [g(x - u, y - v) - \bar{g}]^2 \right\}^{0.5}} \quad (3)$$

with  $\bar{g}$  the mean intensity of the template image and  $\bar{f}_{u,v}$  the mean intensity of the image  $f$  restricted to the region under the template.

The need for a normalization of Equation (2) is mainly due to contrast and brightness irregularities across the reference image, which inevitably alter the global maximum we seek [8].

### 2.1.3 Template matching implementation

We used the `scipy` library implementation of 2d cross-correlation function ‘`correlate2d`’. The following describes the process to achieve template matching using the ‘`correlate2d`’ function.

1. Load the reference image and the template image.
2. Subtract by the mean and divide by the standard deviation for each image to normalize them.
3. Calculate the cross correlation using `correlate2D`.
  - (a) Pad the reference image with a border of width equal to half the size of the template image as shown in Figure 1. That border contains values depending on the boundary condition the user chose. The middle of the template can then reach every pixel of the reference image.

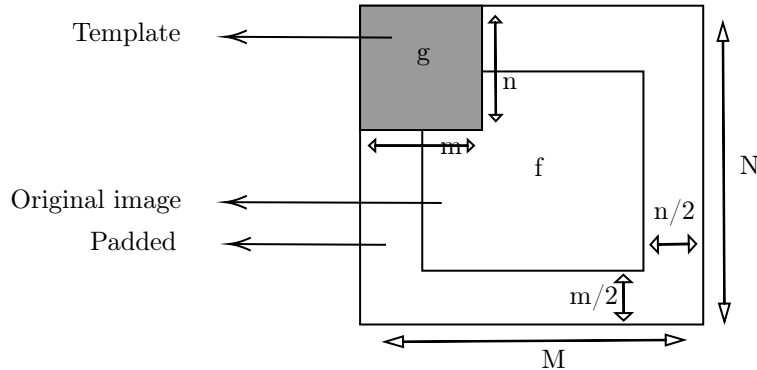


Figure 1: Template matching of a template  $g$  onto a reference  $f$

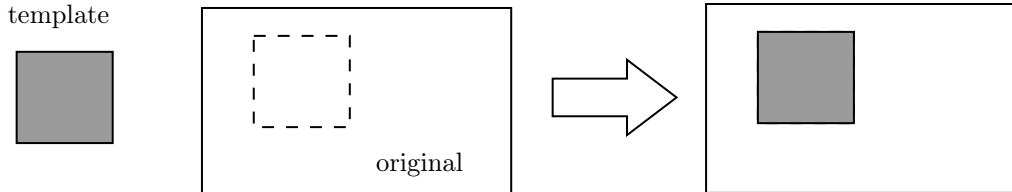


Figure 2: Template matching

- (b) Calculate the cross correlation on each pixel of the reference image.
- (c) Return the cross correlation as an array of the same size as the reference image.
4. Find the indices (coordinates) where maximum is reached on the cross correlation array.
5. Put the template in the matched location by placing its center in the previously found coordinates.

In the next section we explain how we use template matching to create an accurate vector field representing displacement between two images of same size.

## 2.2 From template matching to displacement field

### 2.2.1 Creating a vector field from multiple template matching results

Let us consider two images  $\mathcal{P}$  and  $\mathcal{T}$  of size  $M \times N$ , with  $\mathcal{P}$  being the reference image and  $\mathcal{T}$  an image representing some compensating function coefficients. Generating a displacement field using the previous template matching can be summarized in two steps.

First, we divide our data into squared patches.  $\mathcal{T}$  is now represented by a set of patches that we write :

$$\mathcal{T} = [p_1^{\mathcal{T}}, p_2^{\mathcal{T}}, \dots, p_k^{\mathcal{T}}]$$

with  $k$  being the number of patches required to cover all  $\mathcal{T}$ . We now refer to  $p_i^{\mathcal{P}}(u, v)$  as the corresponding patch of  $p_i^{\mathcal{T}}$  in the reference image in terms of location. The choice of the size of the template patches with regard to the reference patches depends on the use-case scenario. In our case, geo-referencing data and ground truth suggest that we find a relatively small displacement [9], which should not exceed 100 meters (worst case, corresponding to 20 pixels with a 5m. per pixel resolution image). Therefore, for each patch  $p_i^{\mathcal{T}}, i = 1, \dots, k$ , we trim borders by 20 pixels, which fixes the maximum displacement at 20 pixels in terms of infinity norm. We generalize to any scenario noting  $a$  the maximum displacement allowed. Remark that this part of the process profit from exact a-priori information, but optimal parameter  $a$  can be guessed by adding a credible discrete interval for it to the target variables in Equation 5. Illustration of the patch setup is presented in Figure 4. We define the constraint set  $X$  as :

$$X = \{(u, v) \in \mathbb{R}^2 \mid \|(u, v)\|_{\infty} \leq a\} \quad (4)$$

The second step is then to locate each patch  $p_i^{\mathcal{T}}$  inside its corresponding patch  $p_i^{\mathcal{P}}$  using NCC template matching. By iterating over all patches of the images, we obtain a vector field representation of all the local displacements of  $\mathcal{T}$  with respect to  $\mathcal{P}$  (see Figure 3).

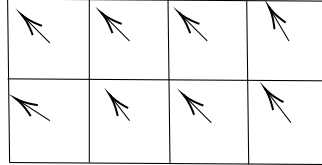


Figure 3: Vector field obtained thanks to patch-wise template matching protocol

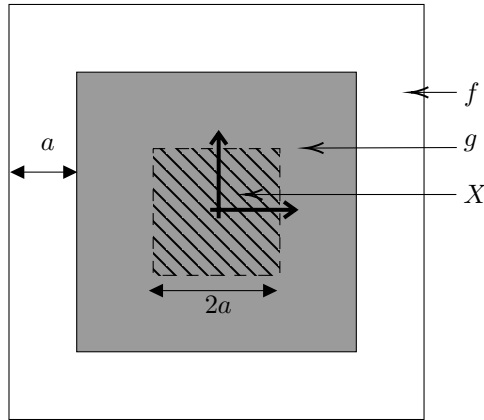


Figure 4: Template matching setting of  $g$  onto  $f$  for a situation with constraint set  $X$

### 2.2.2 Superimpose images with a displacement field

We make the important assumption that the displacement field between  $\mathcal{T}$  and  $\mathcal{P}$  is uniform. We superimpose  $\mathcal{T}$  and  $\mathcal{P}$  by first averaging the vector field (in terms of norm and flow direction) and then applying a linear mapping  $M$  to each pixels of  $\mathcal{P}$ . This linear mapping is defined as :

$$M: \mathbb{R}^2 \rightarrow \mathbb{R}^2$$

$$(x, y) \mapsto (x + u^*, y + v^*)$$

with  $(u^*, v^*)$  the mean shift between  $\mathcal{T}$  and  $\mathcal{P}$  defined as :

$$(u^*, v^*) = \arg \max_{(u, v) \in X} D(\mathcal{T}, \mathcal{P}, u, v) \quad (5)$$

$D$  being a similarity indicator we write as :

$$D(\mathcal{T}, \mathcal{P}, u, v) = \sum_{i=1}^k \gamma(p_i^{\mathcal{T}}, p_i^{\mathcal{P}}, u, v) \quad (6)$$

and where  $\gamma$  is the NCC function defined in Equation (3). We clearly see that if the displacement field is not uniform we introduce error when averaging over all patches in Equation (5).

In the case where  $\mathcal{T}$  represents a compensating function, we divide the newly shifted  $\mathcal{P}$  image intensity by the  $\mathcal{T}$  image intensity and we obtain the compensated  $\mathcal{P}$  image. In the following sections we consider  $\mathcal{P}$  to be the SAR intensity image and  $\mathcal{T}$  the DEM image. We also refer to compensated SAR intensity images as  $i^0$  regardless of the method of matching used.

### 2.2.3 Overlapping patches for improved accuracy

For more precise results we also implement a version with overlapping patches. The overlap factor is a variable that can be changed by the user.

The overlapped patch path makes it possible to keep the accuracy of the correlation calculation, while considerably increasing the number of vectors. The overlap factor allows for an efficient adjustment of the field sharpness.

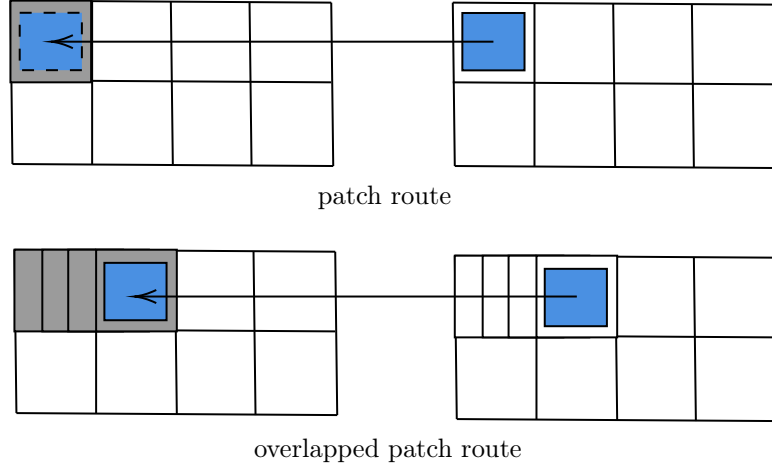


Figure 5: Template matching protocol

Note that if your images differ only up to a uniform translation, as in this paper, results will not profit from a high overlapping factor as the calculation time become too high compared the potential improvements.

### 3 Study case of the Paracou test site with TropiSAR data

#### 3.1 Test site features

TropiSAR data were used to test both implementation and relevance of our approach, given that these P-band data provide a very realistic scenario to prepare the upcoming BIOMASS mission. The TropiSAR airborne campaign aimed to assess P-band utility on AGB retrieval of dense forest [9]. It operated over the Paracou experimental station located in French Guiana. This site is characterized by its hilly topography, which is interesting to study ground compensation techniques. Topography data was provided by SRTM Digital Elevation Models (DEM) (see Figure 6b) [9]. To complete airborne and spaceborne data, in situ data is provided in 15 ground plots of 250mx250m (6.25 ha) and one ground plot of 500mx500m (25 ha) located in the south east of Paracou (see Figure 6a). AGB measurements in these regions of interest (ROI) range from 260 to 430 t/ha.

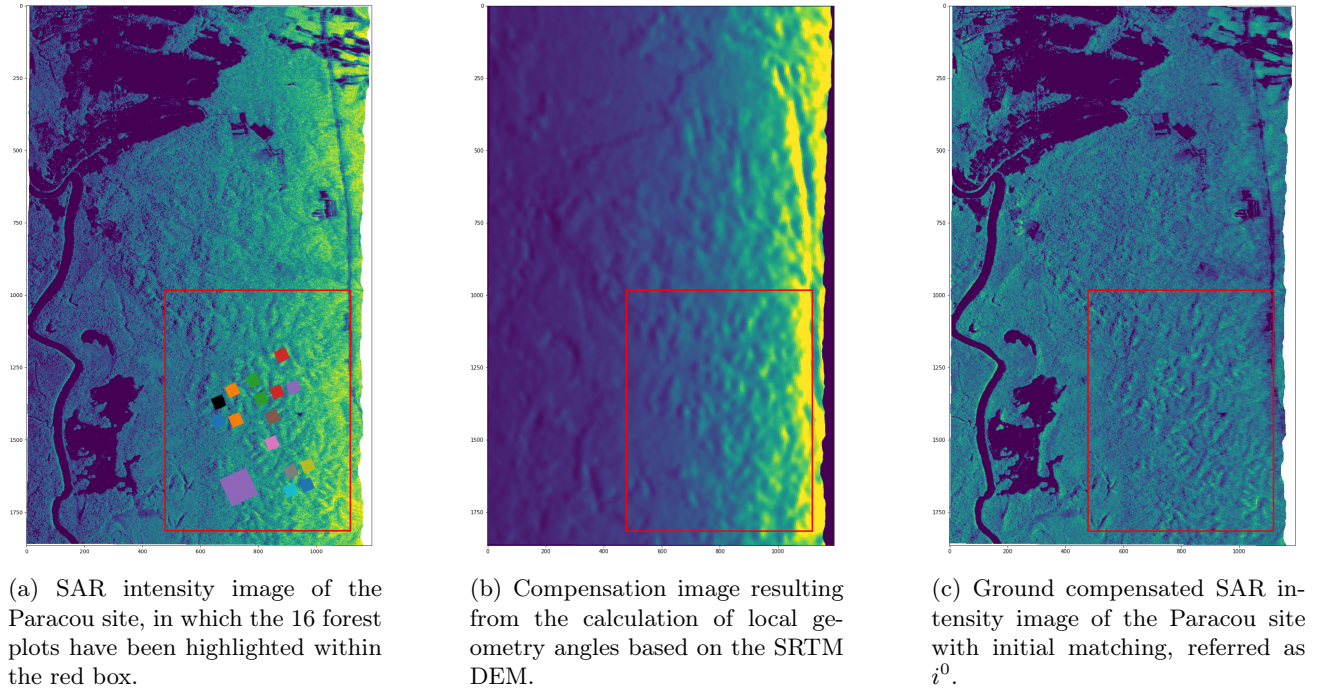


Figure 6: Experimental data from TropiSAR data and initial compensation image based on angles calculation from SRTM DEM.

The higher intensity on the right side of the SAR intensity and DEM images accounts for radar effects, due to the airborne route and incidence angle of the radar over the Paracou site (more details in [9]). The initial matching achieved by dividing the SAR intensity image by the DEM image without applying any translation to the images produce a compensated SAR intensity image (see Figure 6c) in which radar effect are already strongly minimized.

#### 3.2 Matching DEM image and SAR intensity image

We restrict ourselves in the south east region of the Paracou site, where all forest plots are located, highlighted with a red box in Figure 6a, to perform the matching process. We refer to this area as the focus zone in the rest of this paper. After applying image matching we obtain a uniform displacement field as shown in Figure 7a. We recall that the more uniform the vector field is, the less error we introduce when calculating

mean displacement with Equation (5). We calculate the mean displacement and apply translation to the SAR intensity image which led us to the optimized  $i^0$  image seen in Figure 7c. Figure 7b consists in initial matching  $i^0$  image shown in Figure 6c trimmed to the focus zone.

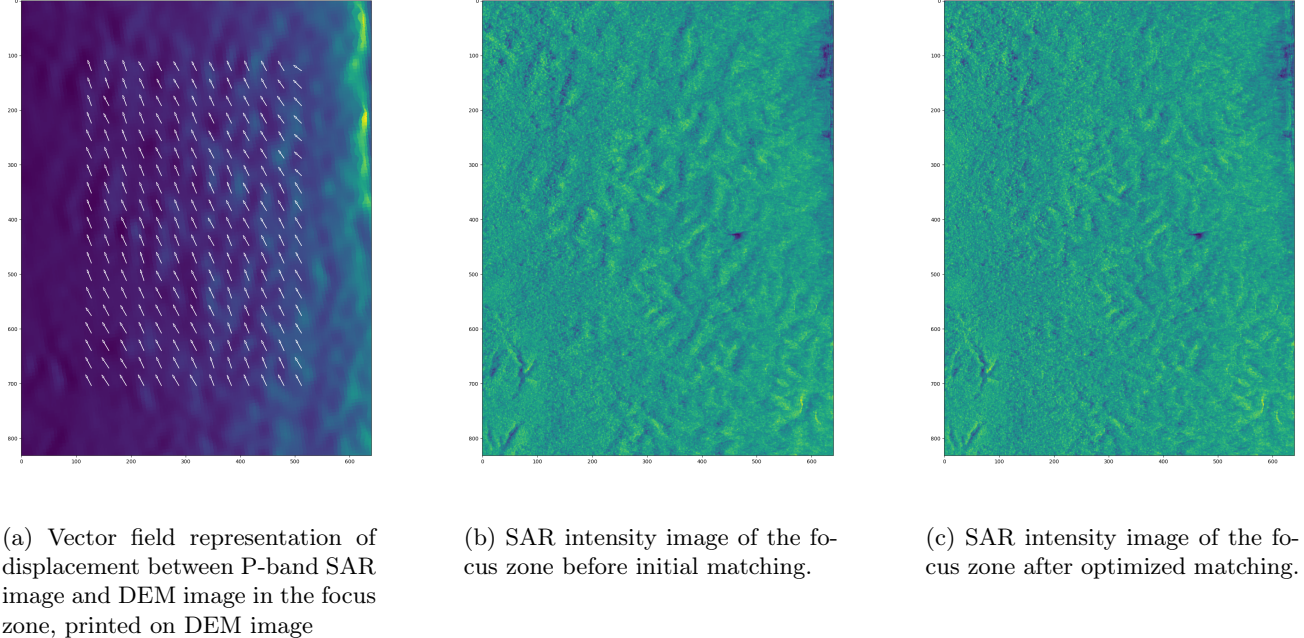


Figure 7: Experimental results and comparison of initial and optimized matching of P-band SAR image with DEM image in the focus zone.

Figure 7 features a comparison of the initial matching  $i^0$  image (see Figure 7b) result with the optimized matching  $i^0$  image (see Figure 7c). We see clearly how optimized matching does a better job reducing terrain asperity: Figure 7c appears much less hilly. Image matching parameters used for the matching results shown in Figure 7c are described in Table 1.

Table 1: Parameters used for optimized matching results presented in Figure 7a

Resolution	Patch size	Overlap
5 m.	256px	8

To minimize uncertainty in our matching method, we use two different resolutions for P-band SAR intensity images : 10m. and 5m. per pixel. Our experiments have shown consistency across these two resolutions as shown in Table 2

Table 2: Image matching results for two different resolutions

Resolution	Patch size	Overlap	$\ (u^*, v^*)\ _\infty$
5 m.	256px	2	15px
10 m.	128px	2	7px

Mean shift ( $\|(u^*, v^*)\|_\infty$ ) for a 2 times lower resolution is approximately divided by two which is coherent and improves confidence on the method consistency.

### 3.3 Estimating image matching impact on SAR intensity to AGB correlation

It is shown in [10] that cross polarized P-band backscatter intensity relationship with AGB is modeled by the following power law.

$$i^0[dB] = a_1 \log_{10}(AGB[t/ha]) + a_0 \quad (7)$$

We can assess the quality of our image matching method by evaluating how  $i^0$  image intensity behaves with regard to AGB. AGB data is provided by forest plots measurements, presented in Section 3.1. Figure 8 shows the relationship between ground compensated P-band backscatter intensity (in dB) in forest plots locations with in situ AGB data in two cases : with 16 ground plot AGB measurements (see Figure 8a) and with 85 ground plot AGB measurements (see Figure 8b).

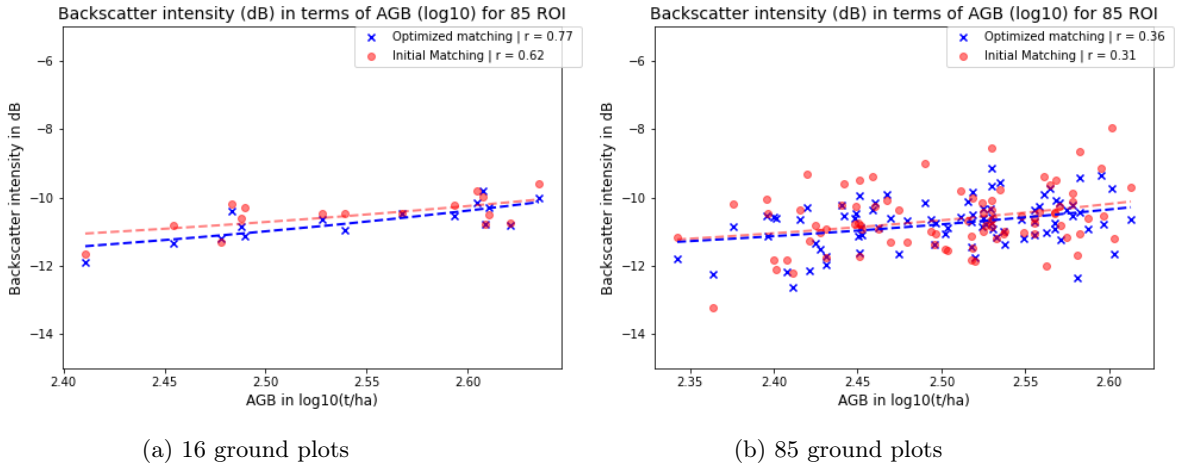


Figure 8: P-band backscatter intensity (dB) in terms of AGB  $\log_{10}(t/\text{ha})$

In case (a) with 16 ground plot measurements, optimized matching  $i^0$  data yields a 0.77 Pearson correlation coefficient while initial matching  $i^0$  data yields a 0.62 coefficient. It translates to a 24% increase in correlation. Case (b), with 85 ground plot measurements, provides a lower but still significant 16% increase in correlation. Optimized matching  $i^0$  intensity correlation coefficient is 0.36, initial matching  $i^0$  data gives us a 0.31 correlation coefficient. However, still in case (b) we note a drop in dispersion with optimized matching  $i^0$  intensity which standard deviation is 0.69 when it is 0.88 with initial matching  $i^0$  data. This drop is not significant in case (a).

The results obtained (Pearson correlation coefficient  $r_P$  increase of 15-24%) are promising. The closer this coefficient is to 1, the more confidently and accurately we can estimate the real amount of biomass with backscattered intensity using the empirical power-law model described in Equation (7). We refer to a Bravais-Pearson coefficient table to assess for Pearson correlation coefficient significance. Given a risk  $\alpha$ ,  $r_P$  must exceed the table value at the appropriate threshold and degree of freedom. Thus, for the sample of  $n = 16$  ROI  $r_P$  must exceed 0.47 for the correlation to be significant, with a 5% risk of error. For the sample of  $n = 85$  ROI  $r_P$  must exceed 0.21. As the results obtained are well above these thresholds, it can be confirmed that the variables are highly correlated hence asserting the validity of the 16-24% increase.

### 3.4 Tuning parameters

#### Adapting patch size

The dimensions of the patches are power values of 2 for practical reasons. One might think that it is possible to densify the displacement field by choosing smaller patch sizes. However, since the data are too different the results become more inconsistent the smaller the patch sizes become. The largest patches tested are 256 pixel patches and these give the best results.

The choice of patch size must be a compromise between sufficiently precise results (sufficiently large patches) and a sufficiently fine vector field (sufficient number of patches). The precision obtained with large patches does not allow user to choose them as large as desired.

#### Coarse shift correction during pre-processing

It appears after experimentation that an initial shift between the two images can distort the results obtained by 'correlate2D'. A routine can be created to find the global shift to be applied on one of the two images for satisfactory results. This routine minimizes the number of aberrant shifts obtained by the 'correlate2D' function but it strongly dependant of your data and may be useless.

#### Bloc route parallelization

The parallelization of the vector field calculations greatly reduces algorithm execution time. The patch route method allows easy parallelization because each template matching is independent of the others. However it is assumed that it is still possible to greatly improve this calculation speed using other parallelization techniques such as cache blocking [11].

## 4 Conclusion and further prospects

The results obtained with this method are promising because we obtain good matching even if the difference between the two images being matched is large. It should be kept in mind that it is sometimes impossible to derive anything from the data available to us, even if we are certain of the expected result. In the case of this matching SAR intensity images and DEM images, the two can be so different that it is impossible to find a perfect displacement field nonetheless we can find a coarse approximation of the desired solution.

Results also allow for an automated process. In this way, the algorithm anticipates the massive processing of satellite data for the upcoming BIOMASS mission. However, there are still a few points to be explored to improve this method:

- Post-processing can be optimised. A coarse approximation of the topographic image shift is made by averaging the vector field displacements and could be improved by introducing elastic image registration techniques, described in [12].
- This approach can be applied to other compensation indicators than  $i^0$ . Finding those indicators is a very active field of research.
- In the context of massive image processing, the code requires an optimized parallelization. This subject has been partly treated using the MPI library of python and has already given very satisfactory results to limit the time required to compute the displacement field.

- This study is limited to a single area of forest. For a greater robustness of the method, its efficiency should be tested in other sites. It is certain that the BIOMASS mission will process data corresponding to a wide variety of terrains, either in terms of forest type or relief.
- The results obtained relate to a particular area that contains only forest. The method shows weaknesses in its results when the area under consideration contains both forest and aquatic areas for example. For massive image processing, one can be interested in detecting a forest area on an image to overcome this difficulty. The reliability of P-Band for non-forested areas should also be investigated.

In this paper we present a simple method to achieve ground compensation on SAR backscatter data in the frame of the future space mission 'BIOMASS'. We develop an image matching method using NCC template matching on overlapped patches of images. We test our method on TropiSAR airborne campaign and in-situ AGB measurements in numerous ground plots. It yields a significant improvement on the Pearson correlation coefficient compared with initial matching data, assessing a better fit to the empirical power-law model. These results were achieved using only one dataset from the Paracou site but suggests that ground compensation can be achieved using simple image registration techniques, thus can be improved greatly.

## 5 Acknowledgment

We would like to thank the Centre National d'Etudes Spatiales (CNES), the Office National d'Etudes et de Recherches Aérospatiales (ONERA) and the Centre d'Etudes Spatiales de la Biosphère (CESBIO) for providing TropiSAR campaign data.

## References

- [1] Shaun Quegan, Thuy [Le Toan], Jerome Chave, Jorgen Dall, Jean-François Exbrayat, Dinh Ho Tong Minh, Mark Lomas, Mauro Mariotti D'Alessandro, Philippe Paillou, Kostas Papathanassiou, Fabio Rocca, Sasan Saatchi, Klaus Scipal, Hank Shugart, T. Luke Smallman, Maciej J. Soja, Stefano Tebaldini, Lars Ulander, Ludovic Villard, and Mathew Williams. The european space agency biomass mission: Measuring forest above-ground biomass from space. *Remote Sensing of Environment*, 227:44 – 60, 2019.
- [2] L. Villard, Thuy Le Toan, D.H. Minh, S. Mermoz, and Alexandre Bouvet. *Forest Biomass From Radar Remote Sensing*, pages 363–425. 09 2016.
- [3] Francesco Banda, Davide Giudici, Thuy Toan, Mauro d'Alessandro, Kostas Papathanassiou, S. Quegan, Guido Riembauer, Klaus Scipal, M.J. Soja, Stefano Tebaldini, L.M.H. Ulander, and Ludovic Villard. The biomass level 2 prototype processor: Design and experimental results of above-ground biomass estimation. *Remote Sensing*, 12:985, 03 2020.
- [4] Ludovic Villard and Thuy Le Toan. Relating p-band sar intensity to biomass for tropical dense forests in hilly terrain: or ? *IEEE Journal of Selected Topics in Applied Earth Observations and Remote Sensing*, 8:214–223, 01 2015.
- [5] F. Zana and J. C. Klein. A multimodal registration algorithm of eye fundus images using vessels detection and hough transform. *IEEE Transactions on Medical Imaging*, 18(5):419–428, 1999.
- [6] P. Marinkovic and R. Hanssen. Advanced insar coregistration using point clusters. In *IGARSS 2004. 2004 IEEE International Geoscience and Remote Sensing Symposium*, volume 1, pages 489–492, 2004.
- [7] Yipeng Hu, Marc Modat, Eli Gibson, Wenqi Li, Nooshin Ghavami, Ester Bonmati, Guotai Wang, Steven Bandula, Caroline M. Moore, Mark Emberton, Sébastien Ourselin, J. Alison Noble, Dean C. Barratt, and Tom Vercauteren. Weakly-supervised convolutional neural networks for multimodal image registration. *Medical Image Analysis*, 49:1 – 13, 2018.
- [8] J.P. Lewis. Fast normalized cross-correlation. *Ind. Light Magic*, 10, 10 2001.
- [9] J. Chave L. Blanc S. Daniel H. Oriot A. Arnaubec M. Réjou-Méchain L. Villard Y. Lasne P. Dubois-Fernandez, T. Le Toan and T. Koleck. “tropisar. technical assistance for the development of airborne sar and geophysical measurements during the tropisar 2009 experiment: Final report”. *Eur. Space Agency, Paris, France*, 2011.
- [10] Michael Schlund, Klaus Scipal, and S. Quegan. Assessment of a power law relationship between p-band sar backscatter and aboveground biomass and its implications for biomass mission performance. *IEEE Journal of Selected Topics in Applied Earth Observations and Remote Sensing*, PP:1–10, 09 2018.
- [11] Muhammad Waqas and Munam Shah. Cache memory: An analysis on optimization techniques. *International Journal of Computer and Information Technology*, 4:414–418, 04 2015.
- [12] J. Kybic and M. Unser. Fast parametric elastic image registration. *IEEE Transactions on Image Processing*, 12(11):1427–1442, 2003.
- [13] Guodong Guo and Charles Dyer. Patch-based image correlation with rapid filtering. 06 2007.